Challenge Journal of Structural Mechanics

Research Article

Performance-based assessment of long masonry structures

Ferit Cakir [a,*]

[a] *Department of Civil Engineering, Gebze Technical University, Gebze, 41400 Kocaeli, Turkey*

ABSTRACT

Performance-based assessment (PBA) has become an increasingly important concept for assessing the structural performance of existing structures today. This procedure aims primarily to determine structural damage subject to predetermined load effects and evaluate the state of the building based on the damage obtained. However, because of their complicated engineering characteristics and structural performance, it is very difficult to evaluate the performance of long masonry structures, such as aqueducts, castle ramparts and city walls. The PBA of long masonry structures is extremely challenging because there is no valid approach to assessing their performance. In this study, a practical evaluation method is developed to assess the structural performance of long structures and the seismic performance of Valens Aqueduct, which was constructed by the Roman Empire in Istanbul, is examined using this method.

ARTICLE INFO

Article history:
Received 23 January 2022
Revised 6 March 2022
Accepted 24 March 2022

Keywords:
Performance-based assessment
Seismic performance
Long masonry structures
Valentine aqueduct

1. Introduction

Masonry structures have been vulnerable to earthquakes by the nature of the brittle materials from which they were built. Therefore, most of the masonry structures built in seismic zones are damaged or collapsed as a result of earthquake effects. To improve the seismic performance of these structures, it is crucial to determine their performance-based seismic performance. For assessing the structural performance of structures, performance-based assessment (PBA) is considered a very important concept. The main objective of this approach is to determine structural damage when predetermined load effects are applied and to evaluate the condition of the building based on the damage obtained. Various standards and codes describe the PBA procedures for different types of structures, such as reinforced or unreinforced masonry structures (ASCE 41-17; FEMA 445-06; FEMA P-58; PERPETUATE-2010). Through linear or nonlinear evaluations, they can be used for assessing existing structures. When conducting seismic performance or damage assessment, several questions must be addressed: a) how to obtain structural drawings, specifically the structural details; b) how to determine the mechanical properties of the construction materials; and c) how to model and evaluate the structures.

How to model and evaluate the structures is the most controversial issue for engineering committees. Many researchers have discussed this topic and masonry structures are modelled and evaluated using several different methods. When the studies in the literature are examined, it is seen that many different building types are evaluated. Cakir (2021) developed a new simplified model to determine the structural performance of masonry structures. Gencer et al. (2020) investigated in-plane and out-of-plane wall behavior due to lateral loading, depending on wall profiles and opening types in Hellenistic towers. Preciado et al. (2015) performed damage analysis of a historic church in Mexico using the nonlinear finite element method. Korkmaz et al. (2015) focused on multi-story masonry structures and evaluated the structural performance of the historical Khatip School in Erzurum, Turkey. Cakir et al. (2015) performed performance evaluations on historical buildings damaged during the 2011 Van earthquake and performed performance analyses on two different historical buildings. Lagomarsino and Cattari (2015) conducted a seismic performance analysis of a historical masonry building using the performance evaluation method developed within the scope of the PERPETUATE project. Brandonisio et al. (2013) evaluated the performance of a masonry church during the 2009 L'Aquila earthquake.

* *Corresponding author*. Tel.: +90-262-605-1000 ; Fax: +90-262-653-8490 ; E-mail address: cakirf@gtu.edu.tr (F. Cakir)
ISSN: 2149-8024 / DOI: https://doi.org/10.20528/cjsmec.2022.02.002

Dogangun and Sezen (2012), considering the 1999 Kocaeli and Düzce earthquakes, examined the seismic performances of five different historical buildings and investigated the seismic weaknesses of the structures. Within the scope of a project called PERPETUATE, a performance-based approach has been proposed by Lagomarsino et al. (2010) for the protection of cultural heritage from earthquakes.

In particular, it is seen that the studies focused on the structures at the single structure scale, but the evaluation studies for the long structures are quite limited. Structures that have a relatively low height and a long length can be considered long structures. The stiffness of these structures is high along with in-plane directions but low along out-of-plane directions. The length of these structures can range from a hundred meters to many kilometers. Aqueducts, castle ramparts, and city walls are the best examples of these kinds of structures (Fig. 1). The evaluation of structural performances of long masonry structures is a very complex issue due to the lack of a valid method for assessing their performance. As part of this study, an evaluation method for the structural performance of long structures was developed, and the seismic performance of the Valens Aqueduct, which was constructed by the Roman Empire in Istanbul, was assessed by using this method.

Fig. 1. Some historical long structures (a) Xi'an City Wall, China; (b) Aurelian Walls, İtaly; (c) Aqueduct of Segovia, Spain; (d) Ávila City Wall, Spain; (e) Osaka Castle Rampart, Japan; (f) Diyarbakır City Wall, Turkey (images from Google Images).

2. Performance-Based Assessment of Long Masonry Structures

In determining the earthquake performance of masonry buildings, a simplified approach based on performance and calculation steps is given in Fig. 2. The PBA of a long structure starts with the seismic hazard assessment of the region and continues with setting the target performance levels and corresponding acceptance criteria, isolating a small segment of the structure, carrying out non-linear analyses on the isolated structure and seismic assessment of the structure.

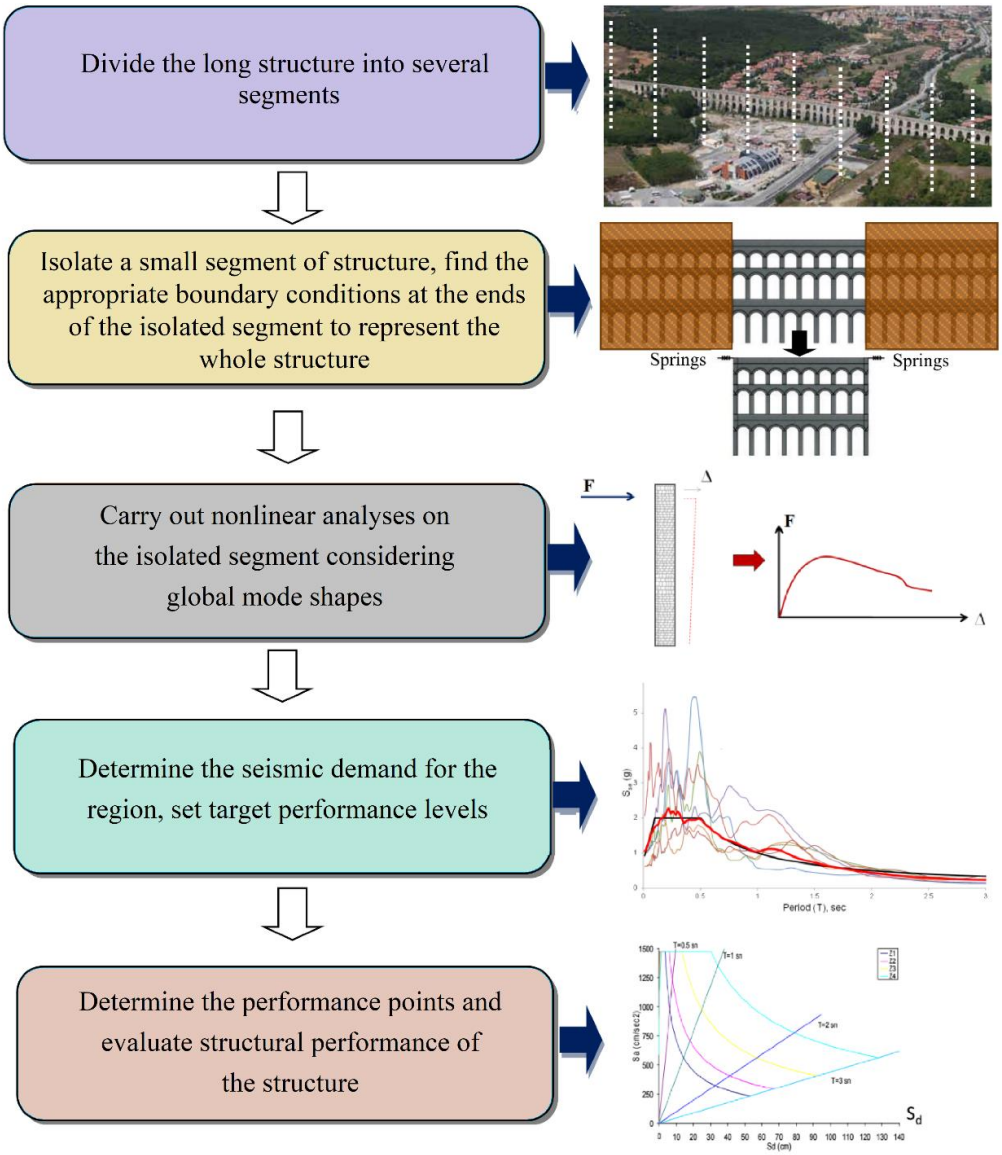

Fig. 2. A layout for performance-based assessment of the long structures.

3. A Case Study: The Valens Aqueduct (Bozdogan Su Kemeri)

3.1. General information

The Valens Aqueduct, which is also known as Bozdogan Su Kemeri, is located in Istanbul, Turkey. The Valens Aqueduct was widely used for supplying water to palaces in history. It stands in the Fatih district of the city and spans the valley between the two hills, which are occupied by Istanbul University and the Fatih Mosque. It was constructed during the late Roman and early Byzantine times. According to historical descriptions, the structure was completed by Emperor Valens (364–378) or Hadrianus (117–138). The aqueduct was later repaired by Emperor Justinian II (576), Konstantinos V (741–775), and Basileios II (1019). During the period of Theodosius II, the aqueduct was used for distributing water to the Baths of Zeus and the Imperial Palace. The structure was restored by Justin II, Basil II and Romanos III. Moreover, during the sovereignty of the Ottoman Empire after 1453, the aqueduct was repaired by Sultan Mehmet II, who was one of the most famous Emperors, and new arches were added to the structure to develop the water supply system. Moreover, the structure was several times restored during the rule of the Ottoman Empire. However, a great part of the Valens Aqueduct was destroyed and only the part located on Atatürk Boulevard has survived (Fig. 3). Although the aqueduct is currently 921 meters long, it was originally 971 meters long, 28.5 meters high and 3.70 meters depth and the aqueduct has 86 different sized arches.

3.2. Performance evaluation

In the performance evaluation, the developed performance-based assessment layout was used and each step in the layout was addressed in detail.

3.2.1. Segmentation and boundary condition

In the scope of the study, the Valens Aqueduct was firstly divided into 125 meters long segments and the segment to be analyzed was isolated. To determine the

stiffness of the springs, two walls were added to the right and left of the isolated segment with the same length as the isolated segment length since it was necessary to express the boundary conditions correctly. The boundary conditions at the ends of the isolated segment can be found by introducing horizontal springs (X and Y directions) at the ends (Fig. 4). Then, the corresponding lateral forces required for a unit displacement of the boundaries for the isolated segment in the X and Y directions were determined by the linear analyses. Finally, these lateral forces were used to determine the lateral stiffness of the springs at the boundaries of the isolated segment. In this model, there are two degrees of freedom spring model was used. In the spring stiffness determination, the force equilibrium equations, Eqs. (1) and (2) were used as follows.

Fig. 3. General views of the Valens Aqueduct (images from Google Images).

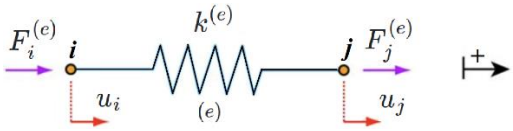

$$k^{(e)}u_i - k^{(e)}u_j = F_i^{(e)} \quad (1)$$

$$-k^{(e)}u_i + k^{(e)}u_j = F_j^{(e)} \quad (2)$$

In matrix form, Eq. (3) was developed.

$$\begin{bmatrix} k^e & -k^e \\ -k^e & k^e \end{bmatrix} \{ \begin{matrix} u_i \\ u_j \end{matrix} \} = \{ \begin{matrix} F_i^{(e)} \\ F_j^{(e)} \end{matrix} \} \quad (3)$$

Since the matrix was symmetric and the order of the matrix was [2×2], the stiffness relation was summarized as Eq. (4).

$$[K^{(e)}]\{u^{(e)}\} = \{F^{(e)}\} \quad (4)$$

where $K^{(e)}$ is the element stiffness matrix, $u^{(e)}$ the nodal displacement vector and $F^{(e)}$ the nodal force vector.

After determining the lateral stiffness of the springs, the structure was discretized with 455210 solid elements with corresponding 1985972 nodes (Fig. 5). In the finite element model (FEM) and finite element analysis (FEA), a general-purpose finite element program, ANSYS Workbench, was used and the isolated segment was numerically modelled with SOLID65 elements, which have eight nodes and three degrees of freedom per node.

In this study, material properties are determined taking into consideration previous studies and general assumptions are made because of the complexity involved in the determination of the material properties (Table 1). In this study, Drucker-Prager Strength Piecewise nonlinear criteria were considered for the nonlinear behavior of the masonry material (Table 2).

Table 1. Mechanical properties of the material.

Property	Value
Density	2300 kg/m³
Young's Modulus	3E+10 Pa
Poisson's Ratio	0,18
Bulk Modulus	1.5625E+10 Pa
Shear Modulus	1.2712E+10 Pa
Max. Tensile Pressure	-4E+6 Pa
Fracture Energy Gf	100 Jm²

Table 2. Drucker Prager strength data.

Pressure (Pa)	Yield Strength (Pa)
0	1E+7
1.5E7	4E+7
5E+7	4.4E+7

Fig. 4. Dividing the structure into segments.

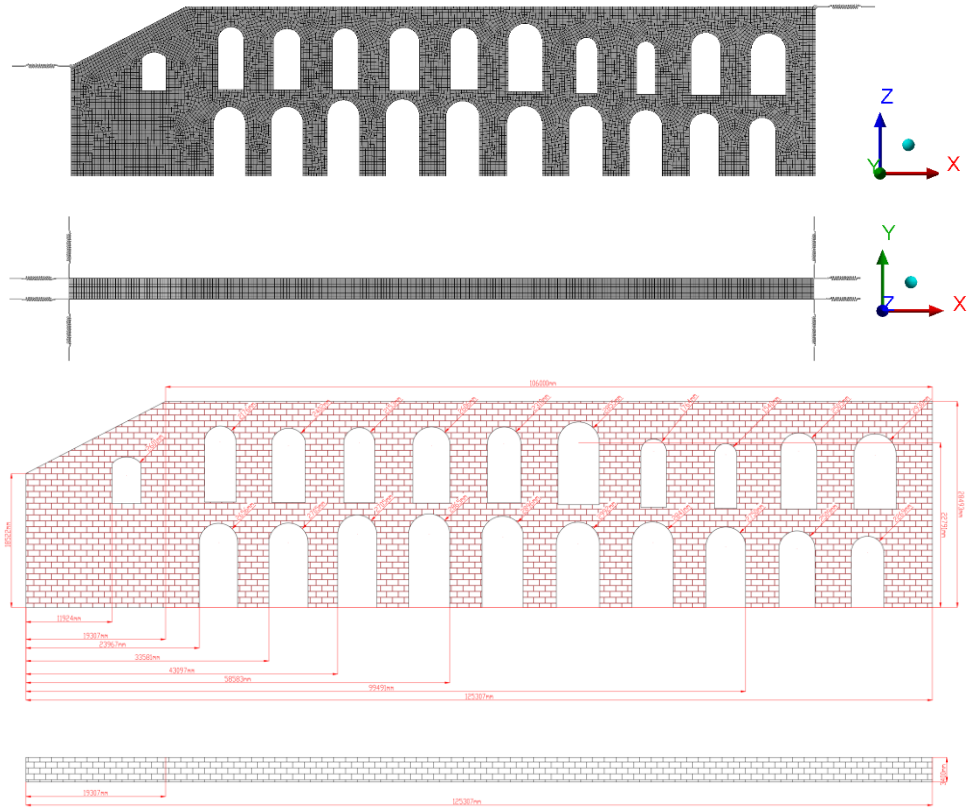

Fig. 5. Numerical model and dimensions of the aqueduct.

3.2.2. Eigenvalue analysis and mode shapes

Modal analysis was performed to determine the dynamic characteristics and seismic behavior of the structure. The modal analysis was conducted including 30 modes and the mass participation ratio in the 30th mode was above 90% in the X and Y directions. The corresponding periods and mass participation ratios obtained with the modal analysis are summarized in Table 3 and the first eight mode shapes of the structure are given in Fig. 6. According to the findings, the first mode and seventh mode were global modes. These global modes constituted an effective mass ratio of more than 71% and 51% in the X and Y directions, respectively. Therefore, in the pushover analysis, the global modes were taken into account and the incremental static analyses in the X and Y directions were performed according to the displacement form in these modes.

3.2.3. Nonlinear static analysis (pushover analysis)

The seismic performance of the structure was investigated through pushover analysis conducted on the finite element model in the X and Y directions. The nonlinear static analysis was made using an incremental-iterative procedure and the analysis procedure adopted in the FEMA 440 and EC-8. To fully define the behaviour in the global modes, the deformation curves of these modes were determined and pushover analysis was performed using these curves (Fig. 7).

Table 3. Frequencies and modal mass participation.

Mode Shape	Frequency (Hz)	Mass Participation Ratios		
		X	Y	Z
Mode 1	2.1878	0.549346E-06	0.509644	0.114848E-10
Mode 2	2.9761	0.124616E-04	0.853842E-03	0.944468E-09
Mode 3	4.3135	0.420495E-07	0.747278E-01	0.102603E-08
Mode 4	5.9585	0.997740E-04	0.803896E-03	0.177276E-07
Mode 5	7.8042	0.947385E-04	0.412953E-01	0.419455E-07
Mode 6	9.8483	0.154870E-01	0.545925E-03	0.619239E-05
Mode 7	10.015	0.713360	0.172893E-03	0.268338E-03
Mode 8	12.111	0.767665E-03	0.714442E-01	0.299998E-06

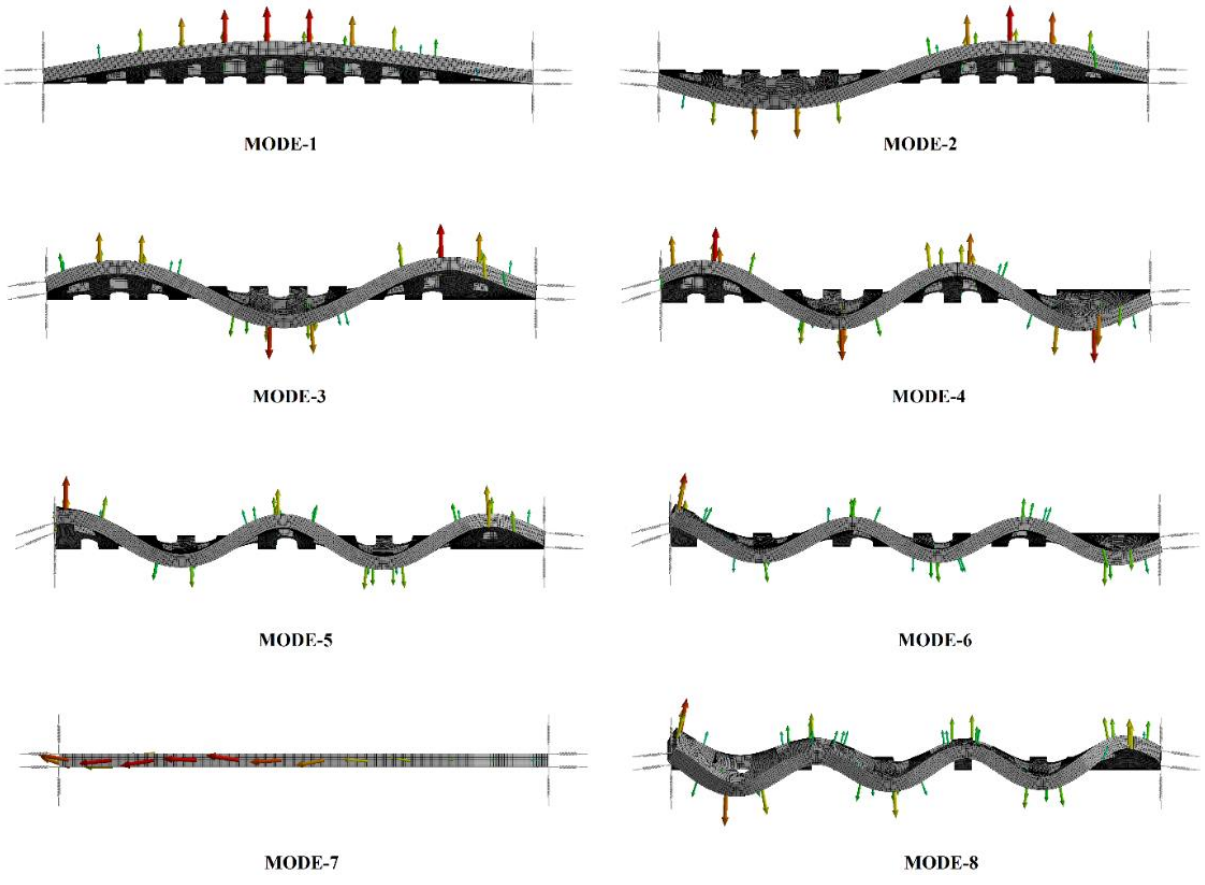

Fig. 6. The first eight mode shapes.

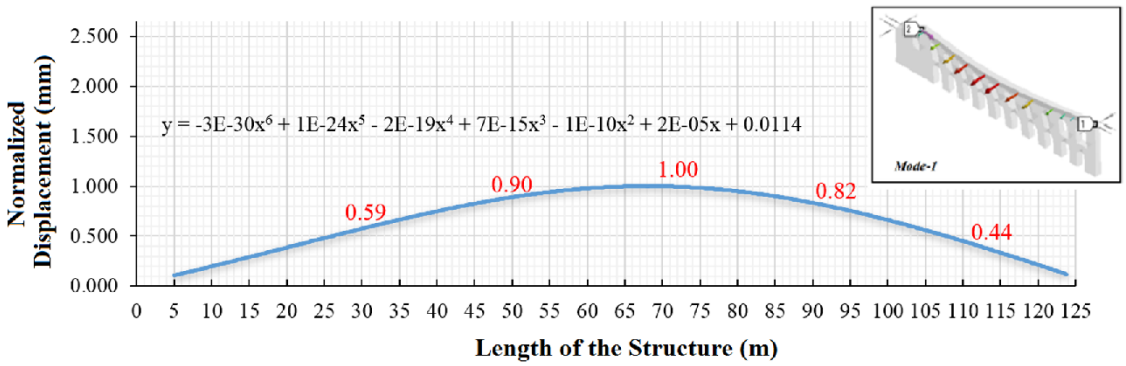

Fig. 7. (continued)

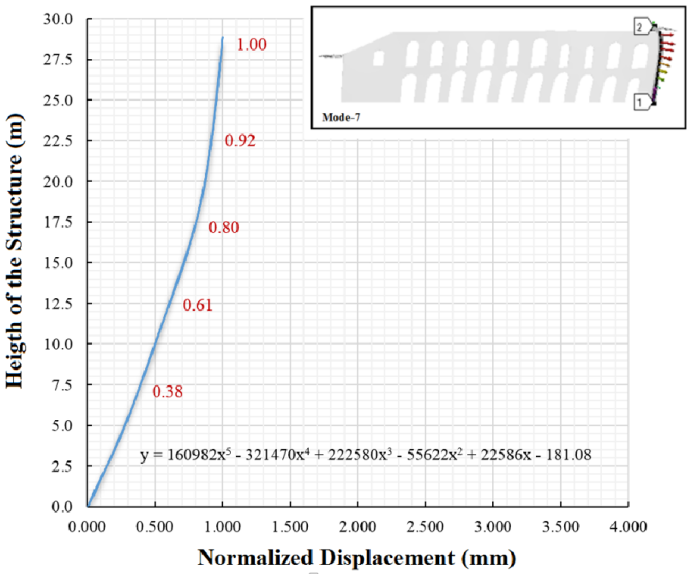

Fig. 7. Normalized displacement pattern obtained from the first and seventh modes.

Based on FEMA 440, in the second phase, the capacity of the structure was determined. The capacity (pushover) curves are plotted in terms of base shear and top displacement. The pushover curve was converted into a modal capacity spectrum by point-by-point conversion of the capacity curve to modal spectral coordinates. Pushover analyses were performed using normalized displacement patterns. In the pushover analysis in the X and Y directions, the equations of the normalized displacement pattern were determined, and incremental static analyses were performed by using these equations. The pushover curves obtained from the pushover analysis in the X and Y directions are presented in Fig. 8a and Fig. 8b, respectively. Then, by using Eqs. (5) and (6) the pushover curves converted to modal capacity curves (Fig. 8c, 8d).

$$a_1^{(i)} = \frac{V_{x1}^{(i)}}{M_{x1}} \tag{5}$$

$$d_1^{(i)} = \frac{U_{xN1}^{(i)}}{\Phi_{xN1}\Gamma_{x1}} \tag{6}$$

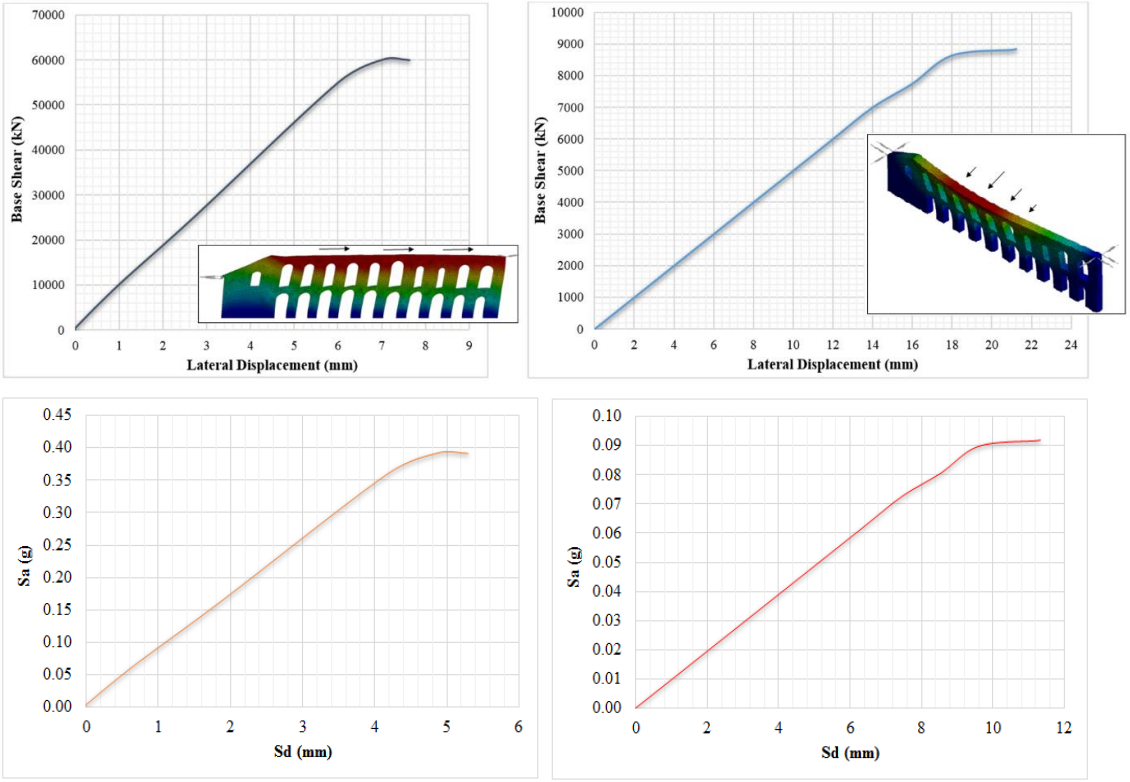

Fig. 8. (a) Pushover curve in the X direction; (b) Pushover curve in the Y direction; (c) Modal capacity curve in the X direction; (d) Modal capacity curve in the Y direction.

3.2.4. Seismic demand

In the seismic demands, two sets of a three-level uniform hazard spectrum; namely, EQ-1, EQ-2, and EQ-3 were constructed using the Turkish Building Earthquake Code-2018 (TBEC, 2018). EQ-1, EQ-2, and EQ-3 for both specifications correspond to the earthquake ground motions with 50%, 10%, and 2% probability of exceedances. EQ-1, EQ-2, and EQ-3 seismic hazard levels were determined using the 5% damped spectral response accelerations at a short period (S_S) and at a period of one second (S_1) are determined for the reference soil type B. The 5% damped spectral response accelerations for short periods (S_S) and at one-second (S_1) for Class B Soil were determined using the site coefficients F_a and F_v. S_S and S_1 were determined as 0.62, 1.19, 1.80 and 0.23, 0.58, 1.02 for EQ-1, EQ-2, and EQ-3 seismic hazard levels, respectively, according to TBEC (2018). F_a and F_v were taken to be 1.0 for EQ-1, EQ-2, and EQ-3 seismic hazard levels, respectively. Both specifications resulted in quite different response spectra in terms of spectral accelerations. Fig. 9a shows the uniform hazard spectra corresponding to these two sets of three-level uniform hazard spectrum. For performance evaluation of the structure, EQ-2 obtained from TBEC (2018) was used as seismic demand due to it is having higher spectral acceleration values at short period region. Then, the response spectrum curve was converted to the demand spectrum by using Eq. (7).

$$S_{ai} = w^2 S_{di} \tag{7}$$

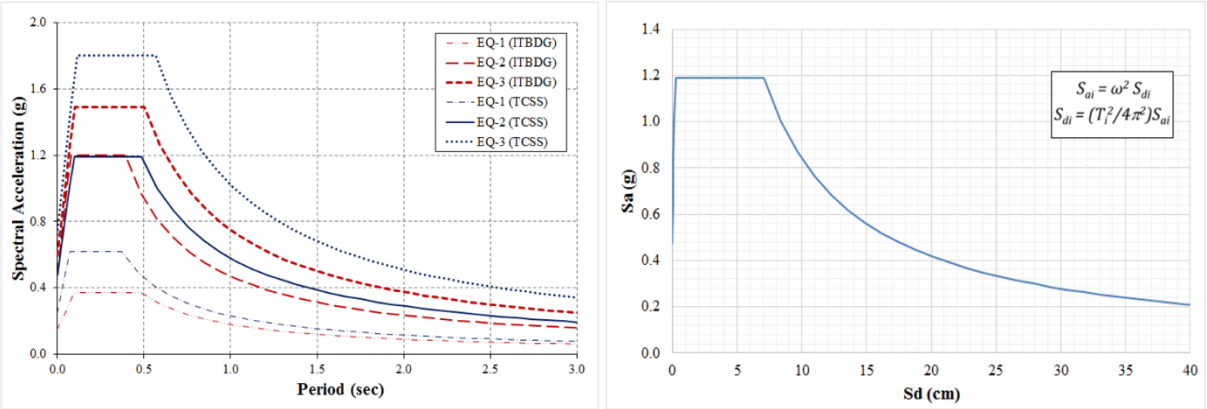

Fig. 9. a) Uniform hazard spectra for the selected seismic hazard levels; (b) Conversion of response spectrum to demand spectrum curve.

3.2.5. Performance evaluation

After the pushover curves were obtained, the coordinate systems were changed to the modal spectrum curves. Then, the modal spectrum curves and seismic demand curves were combined in the same coordinate systems to determine performance points (target displacements) that represent the seismic performance (Fig. 10). Based on the nonlinear static analysis, the target displacement was 10.02 cm in the X direction (in-plane), it was 28.82 cm in the Y direction (out of plane). Top displacements were calculated by using Eq. (8) after the performance points were determined. Top displacements in the X and Y directions are 18.77 mm and 41.58 mm, respectively.

$$u_{xN1}^{(p)} = \Phi_{xN1}\Gamma_{x1}d_1^{(p)} \tag{8}$$

After obtaining the lateral displacement, the drift ratios were determined, and the performance of the structure was evaluated by using the acceptance criteria for URM walls and piers in the current specifications and codes (Table 4). The drift ratio in the X direction (in-plane) was 0.06% while the drift ratio in the Y direction (out-of-plane) was 0.145%.

According to the acceptance criteria, the responses of the Y direction slightly exceeded the immediate occupancy (IO) performance level while the responses of the X-direction remained below the immediate occupancy (IO) performance level. Therefore, it can be said that the performance of the Valens Aqueduct in Istanbul, Turkey is quite good for considered seismic demand. Moreover, as can be seen from Figs. 8a and 8b, it was not possible to laterally push the aqueduct up to these levels of lateral displacements in both directions. The main reason for this was the brittle behavior of the structure. This brittle nature of this masonry structure caused damage during past earthquakes.

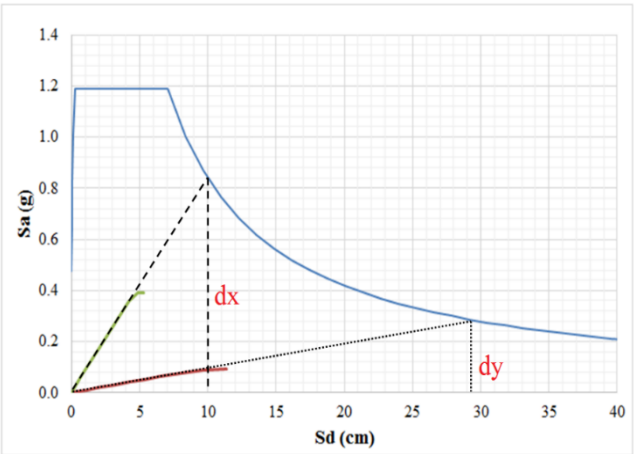

Fig. 10. Performance evaluation.

Table 4. Acceptance criteria for URM walls and piers.

		Primary Members			Secondary Members	
	Limiting Behavioral Mode	Immediate Occupancy (I0) (%)	Life Safety (LS) (%)	Collapse Prevention (CP) (%)	Life Safety (LS) (%)	Collapse Prevention (CP) (%)
FEMA 356 & FEMA 274	Bed-Joint Sliding	0.1	0.3	0.4	0.6	0.8
	Rocking	0.1	0.3 h_{eff}/L	0.4 h_{eff}/L	0.6 h_{eff}/L	0.8 h_{eff}/L
ASCE 41	Rocking	0.1	0.3 h_{eff}/L	0.4 h_{eff}/L	0.6 h_{eff}/L	0.8 h_{eff}/L

h_{eff} = Height to resultant of lateral force

L = Height of wall or pier

4. Conclusions

Masonry aqueducts have been considered to be one of the crucial components of water supply systems throughout history. They are protected with convenient restoration methods and suitable construction materials. The ancient Valens aqueduct studied in this paper was destroyed during past earthquakes and repaired many times in the past. Aqueducts as part of their design have extremely low out-of-plane stiffness compared to the in-plane stiffness. In this study, a practical approach was proposed to assess the structural performance of long historical structures such as aqueducts. This study mainly focused on the numerical modeling and seismic performance of the Valens Aqueduct. A 3D solid numerical model of the structure was constructed and then, the structure was evaluated by the linear and nonlinear analyses. The main outcomes and recommendations obtained from this study are summarized as follows:

- It is not possible to laterally push such brittle structures up to the target displacement when subject to strong earthquake ground motion. The structural behavior is inherently brittle and the structure loses its stability once it starts yielding.
- The past structural damage is consistent with the nonlinear static (pushover) analyses results.
- Since aqueducts are long structures, simple numerical models are needed to understand their structural behavior, because it is almost impossible to model the whole structure. A simple model is proposed in this study. The proposed model is based on isolating a small segment of the structure by introducing linear equivalent springs.
- Long historical masonry structures have a lack of ductility, which is vital from surviving strong earthquake ground motions. Retrofitting schemes for these types of structures should focus on either providing additional lateral strength or ductility.
- Understanding the structural behavior of long historical structures is important in preventing further (progressive) damage and improving their seismic performance.

Acknowledgements

The author would like to thank Prof. Dr. Bulent Akbas for his assistance with the study.

Funding

The author received no financial support for the research, authorship, and/or publication of this manuscript.

Conflict of Interest

The author declared no potential conflicts of interest with respect to the research, authorship, and/or publication of this manuscript.

References

ASCE41-17 (2017). Seismic Evaluation and retrofit of existing buildings, American Society of Civil Engineers. ASCE Standard, ASCE/SEI, 41-17.

Brandonisio G, Lucibello G, Mele E, De Luca A (2013). Damage and performance evaluation of masonry churches in the 2009 L'Aquila Earthquake. *Engineering Failure Analysis*, 34, 693-714.

Cakir F (2021). Tarihi yapıların deprem performansının belirlenmesi için basitleştirilmiş bir yöntem: Kaya Çelebi Cami örneği. *Gazi University Journal of Engineering and Architecture*, 36(3), 1643-1656. (in Turkish)

Cakir F, Uckan E, Shen J, Seker BS, Akbas B (2015). Seismic damage evaluation of historical structures during Van Earthquake, October 23, 2011. *Engineering Failure Analysis*, 58, 249-266.

Dogangun A, Sezen H (2012). Seismic vulnerability and preservation of historical masonry monumental structures. *Earthquake and Structures*, 3(1), 83-95.

EC8-3 (2005). Eurocode 8. 2005. Design of structures for earthquake resistance—part 3: assessment and retrofitting of buildings. EN 1998–3, CEN.

FEMA 440 (2005). Improvement of Nonlinear Static. Seismic Analysis Procedures. Federal Emergency Management Agency (FEMA). Department of Homeland Security (DHS), Washington, D.C.

FEMA 445 (2006). Next-generation performance-based Seismic Design Guidelines, Program Plan for new and existing buildings. Federal Emergency Management Agency (FEMA), Department of Homeland Security (DHS), Washington, D.C.

FEMA P-58 (2018). Seismic Performance Assessment of buildings, volume 1-methodolgy, second edition, Fema P-58-1. Federal Emergency Management Agency (FEMA), Department of Homeland Security (DHS), Washington, D.C.

Gençer F, Hamamcıoğlu-Turan M, Aktaş E (2020). Investigation of in-plane and out-of-plane wall behavior related to lateral loading depending on wall profiles and opening types in Hellenistic Towers. *Gazi University Journal of Engineering and Architecture*, 35(1), 241-253.

Korkmaz M, Ozdemir MA, Kavali E, Cakir F (2018). Performance-based assessment of multi-story unreinforced masonry buildings: The case of historical khatib school in Erzurum, Turkey. *Engineering Failure Analysis*, 94, 195–213.

Lagomarsino S, Cattari S (2015). PERPETUATE guidelines for seismic performance-based assessment of cultural heritage masonry structures. *Bulletin of Earhtquake Engineering*, 13, 13-47.

Lagomarsino S, Modaressi H, Pitilakis K, Bosjlikov V, Calderini C, D'Ayala D, Benouar D, Cattari S (2010). PERPETUATE project: the proposal of a performance based approach to earthquake protection of cultural heritage. *Advanced Material Research*, 133–134, 1119–1124.

Lagomarsino S, Ottonelli D, Cattari S (2019). Performance-based assessment of Masonry Churches: Application to San Clemente Abbey in Castiglione A Casauria (Italy). *Numerical Modeling of Masonry and Historical Structures*, 55–89.

Milani G, Shehu R, Valente M (2017). Seismic performance assessment of three masonry churches through Fe simulations. *AIP Conference Proceedings*, 1863, 450014.

PERPETUATE (2010). Classification of the cultural heritage assets, description of the target performances and identification of damage measures, deliverable D4, performance-based approach to earthquake protection of cultural heritage in European and Mediterranean countries, FP7—Theme ENV.2009.3.2.1.1-Environment, Grant agreement no: 244229, DELIVERABLE D4, June 30, 2010.

Preciado A, Orduna A, Bartoli G, Budelmann H (2015). Façade seismic failure simulation of an old cathedral in Colima Mexico by 3D limit analysis and nonlinear finite element method. *Engineering Failure Analysis*, 49, 20-30.

TBEC (2018). Turkish Building Earthquake Code. Disaster and Emergency Management Presidency (AFAD), March 18, 2018, Ankara.